EurJOC
European Journal of Organic Chemistry

Research Article
doi.org/10.1002/ejoc.202500338

Chemistry Europe
European Chemical Societies Publishing

www.eurjoc.org

A C_3-Symmetric Diphenylethylendiamine-Based Catalyst in the Asymmetric Michael Addition of α,β-Unsaturated Ketones with 4-Hydroxycoumarin and 4-Hydroxyquinolin-2-One

Shilashi Badasa Oljira, Martina De Angelis, Simone Manetto, Francesco Fiorentino, Dante Rotili, Luciana Mosca, Daniel Di Risola, Roberto Mattioli, Marco Pierini, Giulia Mazzoccanti, and Alessia Ciogli*

Even though the amino-organocatalysis has been known for decades, the use of chiral C_3-symmetric multiamino catalysts in asymmetric synthesis is not widespread. Herein, the previously employed approach for the chiral 1,2-diamino-cyclohexane to the enantiopure 1,2-diphenylethylendiamine is extended. The independent activity of each catalytic subunit is also confirmed for this enantiopure motif by offline high-resolution electrospray mass spectrometry (ESI-MS) experiments. The advantages and limitations of this novel approach in the asymmetric Michael addition of α,β-unsaturated ketones to 4-hydroxycoumarin and 4-hydroxyquinolin-2-one, achieving up to 95% yield and moderate-to-good stereocontrol (enantiomeric ratio up to 80:20) are evaluated. In the pool of synthetized molecules, there are two novel compounds, and one is prepared for the first time using organocatalysis. In addition, some of these molecules show an intrinsic scavenging ability on $ABTS^{\bullet+}$ radical.

1. Introduction

Catalytic asymmetric synthesis has become an essential tool for the enantioselective synthesis of active molecules mainly in pharmaceuticals, natural products, and agrochemicals.[1,2] Among the various approaches to asymmetric catalysis,[3–6] the use of chiral organic molecules has attracted significant interest due to structural simplicity, easy availability, low cost, mild reaction conditions, broad functional group tolerance, and their potential as sustainable alternatives to metal-based catalysts.[7,8] C_3-symmetric organic molecules, characterized by a structural moiety repeated three times around a rotational axis, have been widely used as ligands in metal catalysis or molecular acceptors, scaffolds in supramolecular and macromolecular structures, gels oxidizing agents, and more recently in the development of organometallic materials.[9–17] Despite their versatility, the use of these compounds in organocatalysis remains relatively an unexplored field. However, promising examples based on amino groups and amino derivatives arranged in C_3-symmetric shape exist. **Figure 1** reports the structure of C_3-symmetric organocatalysts selected from the literature and information about the reactions where they are involved. For example, Pan et al. successfully applied tribenzyl and triphenylphosphineoxide-based proline organocatalysts for aldol reactions.[18] Moorthy et al. developed C_3-symmetric proline-based and pyrrolidine-based catalyst providing Michael adducts of carbonyl compounds and trans-β-nitrostyrene with high stereoselectivities.[19] Fujioka et al. have developed trisimidazoline derivatives successfully utilized as catalysts in Michael addition reactions, σ-amination of β-ketoesters, and bromolactonization of alkenoic acids.[20,21]

Similarly, C_3-symmetric cinchona-based catalysts were investigated in the asymmetric Michael and Friedel–Crafts reactions.[9] The authors found an increased selectivity of one C_3-arranged catalyst in comparison to hydroquinine in the Michael reaction of pentane-2,4-dione and trans-β-nitrostyrene. Building on these developments, our group recently developed C_3-symmetric

S. B. Oljira, S. Manetto, F. Fiorentino, M. Pierini, G. Mazzoccanti, A. Ciogli
Department of Chemistry and Technologies of drugs
Sapienza University of Rome
pl.e A. Moro 5, 00185 Roma, Italy
E-mail: alessia.ciogli@uniroma1.it

M. De Angelis
Department of Chemistry
Sapienza University of Rome
pl.e A. Moro 5, 00185 Roma, Italy

D. Rotili
Department of Science
Roma Tre University
Viale Guglielmo Marconi 446, 00146 Roma, Italy

D. Rotili
Biostructures and Biosystems National Institute (INBB)
Via dei Carpegna 19, 00165 Rome, Italy

L. Mosca, D. Di Risola, R. Mattioli
Department of Biochemical Sciences "A. Rossi Fanelli"
Sapienza University of Rome
pl.e Aldo Moro 5, 00185 Rome, Italy

Supporting information for this article is available on the WWW under https://doi.org/10.1002/ejoc.202500338

Research Article
doi.org/10.1002/ejoc.202500338

Chemistry Europe
European Chemical Societies Publishing

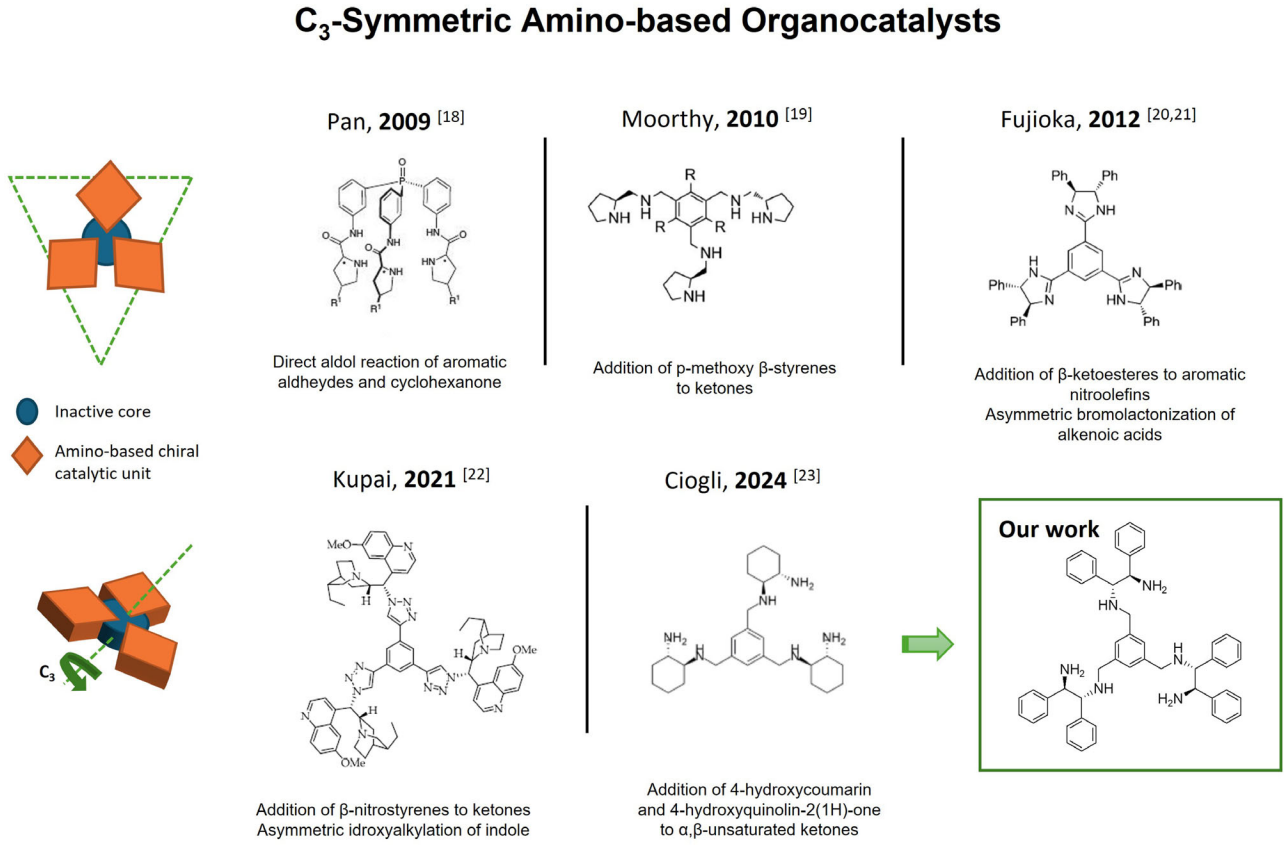

Figure 1. Structures of some C_3-symmetric organocatalysts bearing amino- and amino-derivative groups reported in literature. Below each structure, information about the reactions where they are involved was added.

amino-organocatalysts based on enantiopure trans-1,2-diaminocyclohexane (DACH) for the synthesis of warfarin and its analogues.[22] This study included ESI-MS experiments coupled with density functional theory (DFT) calculation to elucidate the reaction mechanism. As a compelling extension of this approach, we herein present a novel C_3-symmetric catalyst derived from the enantiopure 1,2-diphenylethylenediamine (DPEDA), a widely used building block in organocatalysis due to its versatility in functionalization.[23,24] DPEDA-based organocatalysts have been instrumental in various reactions, including aldol condensations, Mannich, Diels–Alder, desymmetrization, and asymmetric Michael reactions.[23] In particular, the Michael addition of 4-hydroxycoumarin to α,β-unsaturated ketones represents an efficient route for the synthesis of warfarin and its analogs in homogeneous phase as well as by using alternative approaches.[25–32] Usually, existing methodologies often require high catalyst loading (10–20% mol) and acidic co-catalysts to achieve satisfactory yields and stereoselectivities. In this work, extending the idea developed in 2024,[22] we prepared a small library of enantioenriched 4-hydroxycoumarin and 4-hydroxyquinoline derivatives. The evaluation of catalyst performance was also provided in the scaling-up synthesis and in the its potential recycle of one derivative largely used as rodenticide. In addition, the free radical scavenging capacity of novel compounds was measured against $ABTS^{+\cdot}$ species showing a low- to moderate activity.

2. Results and Discussion

The synthesis of the catalyst began with the selective mono-protection of the amino group of chiral (*R*,*R*)-1,2-diamine (**Scheme 1**). Di-tert-butyl dicarbonate (Boc_2O) was used to introduce the Boc protecting group, following a straightforward protocol that provides high yields as described by Kucherenko et al.[7] Specifically, Boc_2O was added dropwise to a solution of trimethylsilyl chloride in methanol. At this step, we evaluated the effect of addition time on yield: extending the dropwise addition time from 10 min to 30 min we obtained increased yield from 65 to 87% of final purified pale-yellow mono-protected diamine **3**. Afterward, following our previous reported protocol,[22] we proceeded with the addition of 1,3,5-benzenetricarbonyl trichloride to mono-Boc DIPEDA **3** in the presence of N-ethyl-diisopropylamine affording 82% of product **4**. The deprotection step using TFA in DCM followed by treatment with the basic resin Ambersep 900-OH, provided the C_3-symmetric amide **6** as free base in excellent yield (98%). The amide **6** was reduced with $BH_3{\cdot}Me_2S$ in dry THF, and followed by the addition of methanol in presence of 1M HCl. The final free base amino-catalyst **7** was obtained after ion exchange through basic resin affording an overall yield of 67%. In the initial screening, we evaluated both catalyst **6**, the amino-amido scaffold, and catalyst **7**, the all-amino one without any acid additive. As well known, the intermediate reactions via imine

Research Article
doi.org/10.1002/ejoc.202500338

Chemistry Europe
European Chemical Societies Publishing

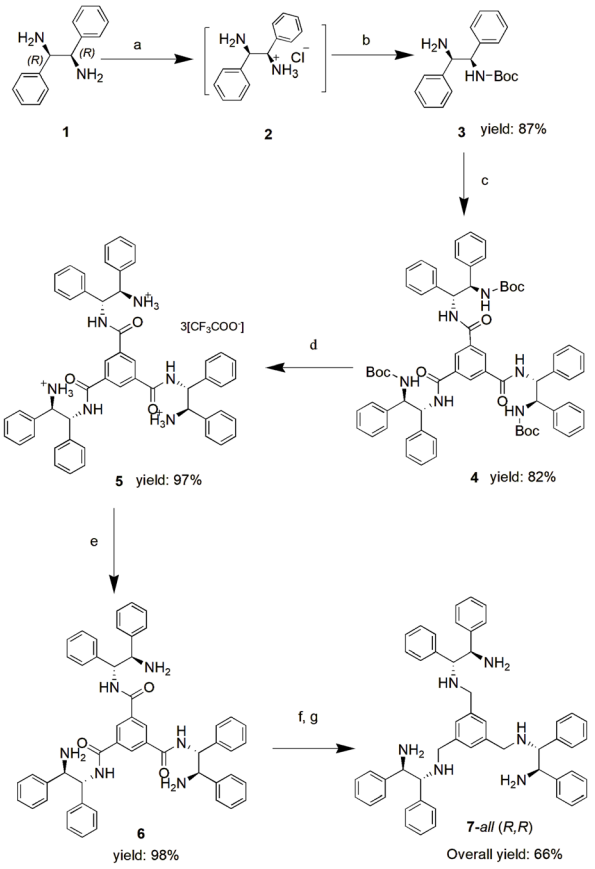

Scheme 1. Synthesis of C_3-symmetric organocatalysts: a) TMSCl, MeOH, 0 °C for 10 min; b) Boc_2O in MeOH dropwise for 30 min, rt for 2 h, yield: 87%; c) 1,3,5-benzenetricarbonyl trichloride, DIPEA, $CHCl_3$ dry, 40 °C for 5 h then rt for 14 h, yield: 82%; d) TFA, DCM, 0 °C, 6 h; e) Ambersep 900-OH 98%; f) $BH_3{\cdot}Me_2S$, THF dry, 80 °C, for 6 h, then rt for 14 h, 1M HCl, MeOH, 80 °C, 8 h; and g) Ambersep 900-OH, 66% yield.

usually require an acid as additive to promote the imine formation. Here, only the 4-hydroxycoumarin **8a** (pKa 4.1) could act as reagents and at the same time as weak acid sources.[33] We started to investigate catalyst activity with 2% mol of catalyst in the reaction between 4-hydroxycoumarin and two different Michael acceptors yielding warfarin (**10a**) and coumachlor (**10b**). This preliminary examination was carried out in THF at room temperature in the presence of 1 equivalent of Michael acceptors **9a,b**. The obtained results are listed in **Table 1**.

The amino-amido catalyst (*all-R*)-**6** afforded the product **10a** and **10b** (entry 1 and entry 2) with a low yield (30% and 43%, respectively) and poor enantiomeric ratio (in term of enantiomeric excess, 22 %e.e. and 28 %e.e., respectively). Moving to (*all-R*)-**7** catalyst, both yield and induced stereocontrol increased up to 70% of the isolated product and to 74/26 of the enantiomeric ratio (56 %e.e.). An increase of catalyst loading (5% mol) furnished the desired **10a** and **10b** products with 87% and 95% yield, respectively, while the induced stereocontrol seems to be less dependent on catalyst loading product (74/26 and 70/30 compared to 78/22 and 76/24, respectively, in terms of the enantiomeric ratio). Similar results in yield, with expected opposite stereochemistry, were obtained by changing the absolute configuration of catalysts (data not shown). These results highlighted the importance of all amino groups in the catalytic process both in terms of yield and stereoinduction, while the presence of amide groups leads to the poor catalytic performances. This agrees with those highlighted for the analogue C_3-symmetric structure based on *trans*-1,2-diamino-cyclohexane.[22] Indeed, by computational conformational analysis, the more stable conformers of (*all-R*)-**6** catalyst endowed with Boltzmann population greater than zero are only two, both characterized by the formation of three intramolecular hydrogen bonds. In depth, each H-bond is established between the primary amino group and the amidic carbonylic oxygen belonging to one of the three framework arms bound to the central benzene cycle, as shown in **Figure 2**. Noticeably, to make the catalyst active, each of three H-bond need to be breached, so that it is foreseeable these may have a partially unfavorable impact on the progress of reaction (see yield of entry 1 and 2 in Table 1).

Table 1. Preliminary screening of catalysts **6** and **7**.

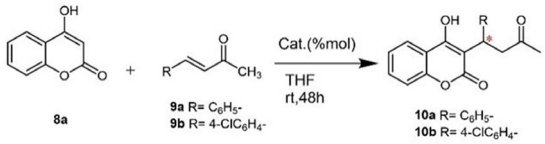

Entry	Ketone	Cat. [% Mol]	Yield [%]	%e.e. *R/S*	Product
1[a)]	C_6H_5-	(*all-R*)-**6**(2)	30	22	**10a**
2[b)]	4-ClC_6H_4-	(*all-R*)-**6**(2)	43	28	**10b**
3[c)]	C_6H_5-	(*all-R*)-**7**(2)	62	48	**10a**
4	4-ClC_6H_4-	(*all-R*)-**7**(2)	70	40	**10b**
5	C_6H_5-	(*all-R*)-**7**(5)	87	56	**10a**
6	4-ClC_6H_4-	(*all-R*)-**7**(5)	95	52	**10b**

[a)]Reactions were performed with **8a** (0.2 mmol), **9** (0.24 mmol), THF (2 mL). [b)]Yield of the isolated product after silica gel column chromatography. [c)]Determined by chiral HPLC analysis.

Research Article
doi.org/10.1002/ejoc.202500338

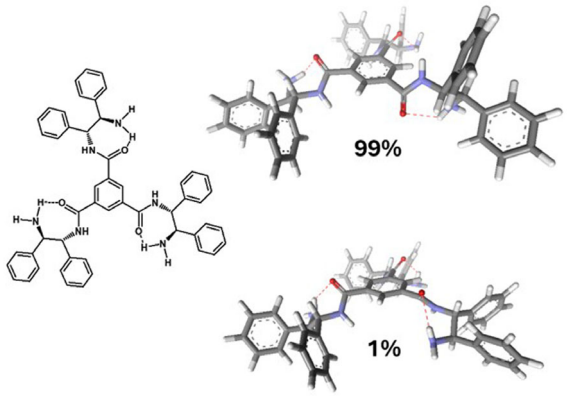

Figure 2. Graphical representation of the computationally optimized structure of catalyst **6** involving intramolecular H-bonds, which may unfavorably act on its catalytic activity.

A similar conformational analysis was also conducted on the structure of (*all-R*)-**7** catalyst, with the aim of evaluating the possible influence that the formation of stable intramolecular H-bonds could have on the related catalytic activity. The obtained results highlighted that the most stable conformation of (*all-R*)-**7** catalyst, characterized by a Boltzmann population of 71%, is devoid of intramolecular H-bond formation and it has a C_3 symmetry axis. An indirect confirmation of this, unlike what was found for catalyst **6**, is that in the main catalyst **7** conformer, the amino groups are not potentially inhibited by the formation of H-bond and can therefore be more easily involved in the catalytic activity, was obtained by computationally optimizing this conformation in the presence of both one hydroxyquinoline **8a** and one ketone **9a** molecules (see Table 1). The presence of this couple of reagents leads to an easy change of conformation of catalyst **7** promoted by the establishment of very favorable intermolecular H-bonds.

Furthermore, four independent transition states, TSs, were assembled by hand and optimized at the PM6 semiempirical level of theory (namely, by the acronym $\mathbf{TS_a}$, $\mathbf{TS_b}$, $\mathbf{TS_c}$, and $\mathbf{TS_d}$). The TSs correspond to the first reaction step involved to the synthesis of **10a** (the formation of the carbinolamine between (*all-R*) catalyst **7** and ketone **9a**, promoted by the acidic support of hydroxyquinoline **8a**), all confirmed by the presence within each of their simulated infrared (IR) spectra of only one imaginary frequency. The structures of calculated transition states were reported in Figure S30, Supporting Information. Interestingly, already at this initial level of reaction progress by the performed calculations was possible to validate the experimentally found catalytic stereoselectivity. Indeed, two of the carbinolamine intermediates resulting by the overcoming of the relative $\mathbf{TS_a}$ and $\mathbf{TS_b}$ show to expose the ***Re*** enantiotopic unsaturated face to the subsequent and necessary nucleophilic attack of the hydroxycoumarin **8a**, while the other two, $\mathbf{TS_c}$ and $\mathbf{TS_d}$, expose the ***Si*** enantiotopic unsaturated face. As a result, in the first case (attack of **8a** on the ***Re*** face) in the final product **10a** the configuration of the chiral atom will be ***R***, while in the second one (attack of **8a** on the ***Si*** face) the resulting configuration will be ***S***. Looking to the TS energy content, among the above cited four $\mathbf{TS_a}$, $\mathbf{TS_b}$, $\mathbf{TS_c}$, and $\mathbf{TS_d}$ ($\mathbf{TS_a}^{Energy} = 329.05$ KJ, $\mathbf{TS_b}^{Energy} = 324.92$ KJ, $\mathbf{TS_c}^{Energy} = 331.11$ KJ, $\mathbf{TS_d}^{Energy} = 337.77$ KJ), the two more stable ones, $\mathbf{TS_a}$ and $\mathbf{TS_b}$, are characterized by exposing the enantiotopic unsaturated face ***Re*** to the attack of **8a**, while the third and four, $\mathbf{TS_c}$ and $\mathbf{TS_d}$, the face ***Si***, in agreement with the experimentally observed prevalence in the final product **10a** of the ***R*** configuration over the ***S***. In **Figure 3** the most stable TSs for the two different Re and Si faces are reported. The prevalent energetic stability of the **TS** structure, inducing on **10a** the ***R*** configuration, over the one inducing instead the ***S*** configuration was also confirmed by submitting all the $\mathbf{TS_a}$, $\mathbf{TS_b}$, $\mathbf{TS_c}$ and $\mathbf{TS_d}$ geometries to single point energy calculations at the much more high Density Functional level of Theory (DFT, see Supporting Information for further details).

2.1. Reaction Scope

The catalytic capability of (*all-R*)-**7** was evaluated by synthesizing a small library of warfarin analogues. All reactions were performed

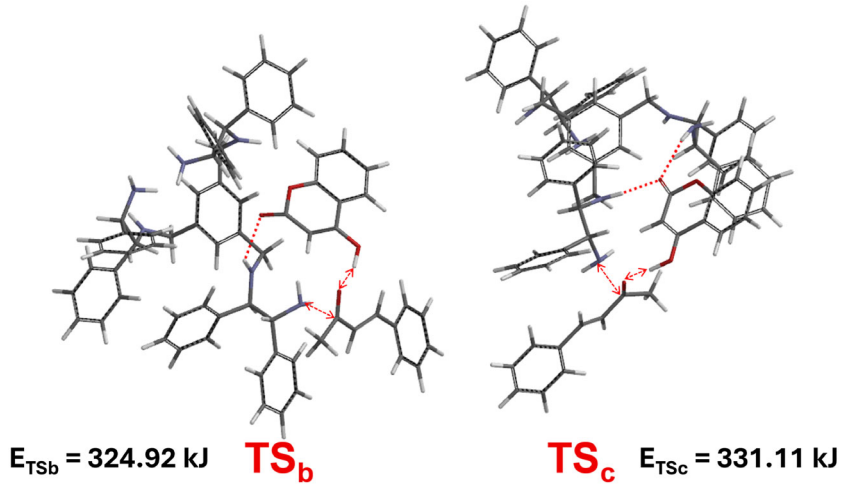

Figure 3. Graphical representation of the computationally optimized structure of more stable transition states TS_b and TS_c exposing *Re* and *Si* faces, respectively. The other two TSs were in Supporting information (Figure S30).

Research Article
doi.org/10.1002/ejoc.202500338

Chemistry Europe
European Chemical Societies Publishing

using 5% mol of catalyst at room temperature. Various α,β-unsaturated ketones **9** were employed in combination with the two cyclic Michael donors **8a** and **8b**. The reactions were carried out in distinct solvents: THF was used for reactions with **8a**, while DMSO, for solubility reasons, was employed for those involving **8b** as the reagent.

The corresponding products **10c–i** were obtained from low to moderate yields with good enantioselectivities (**Figure 4**). In fact, in all products achieved with 4-hydroxycoumarin, the enantioselectivity ranges from 80/20 to 70/30, seeming not affected by the nature of ketone substituent. Instead, when 4-hydroxyquinolinone **8b** was used, all reactions provided products with different enantiomeric ratios (from the *quasi-racemic* product of **10h** to the 78/22 enantiomeric ratio of **10c**).

This revealed that both types of heteroatoms in the Michael donors and the nature of substituents have an impact on the catalytic performance. Notably, the presence of oxygen or nitrogen seems to affect the stereoselectivity more than the structure of the substituent (see pairs **10e/10f** and **10g/10h** in Figure 4). However, the stereoselectivity remains consistent between **10a/10c** and **10b/10d** pairs, where the methyl group in R_2 is maintained. Although the last three reactions did not give exciting yields, **10h** and **10i** have been synthesized as new compounds and they were resolved through enantioselective HPLC by using double circular dichroism (CD)/UV detection or the inverted chiral column approach to discriminate the enantiomeric pair (Supplementary Information).[34] The compound **10g**, already known, has been prepared for the first time through asymmetric aminocatalysis. In literature, to our knowledge, **10g** has been synthetized in asymmetric version by metal-assisted catalytic reactions, whereas other examples report the efficacy and innovative approaches for racemate production.[35–37]

2.2. Investigation of Catalytic Cycle by HR-ESI-MS

To confirm the catalytic activity of multiple amine units, we performed high-resolution (HR) ESI-MS studies.[38–41] We identified the most relevant intermediates by off-column flow-injection

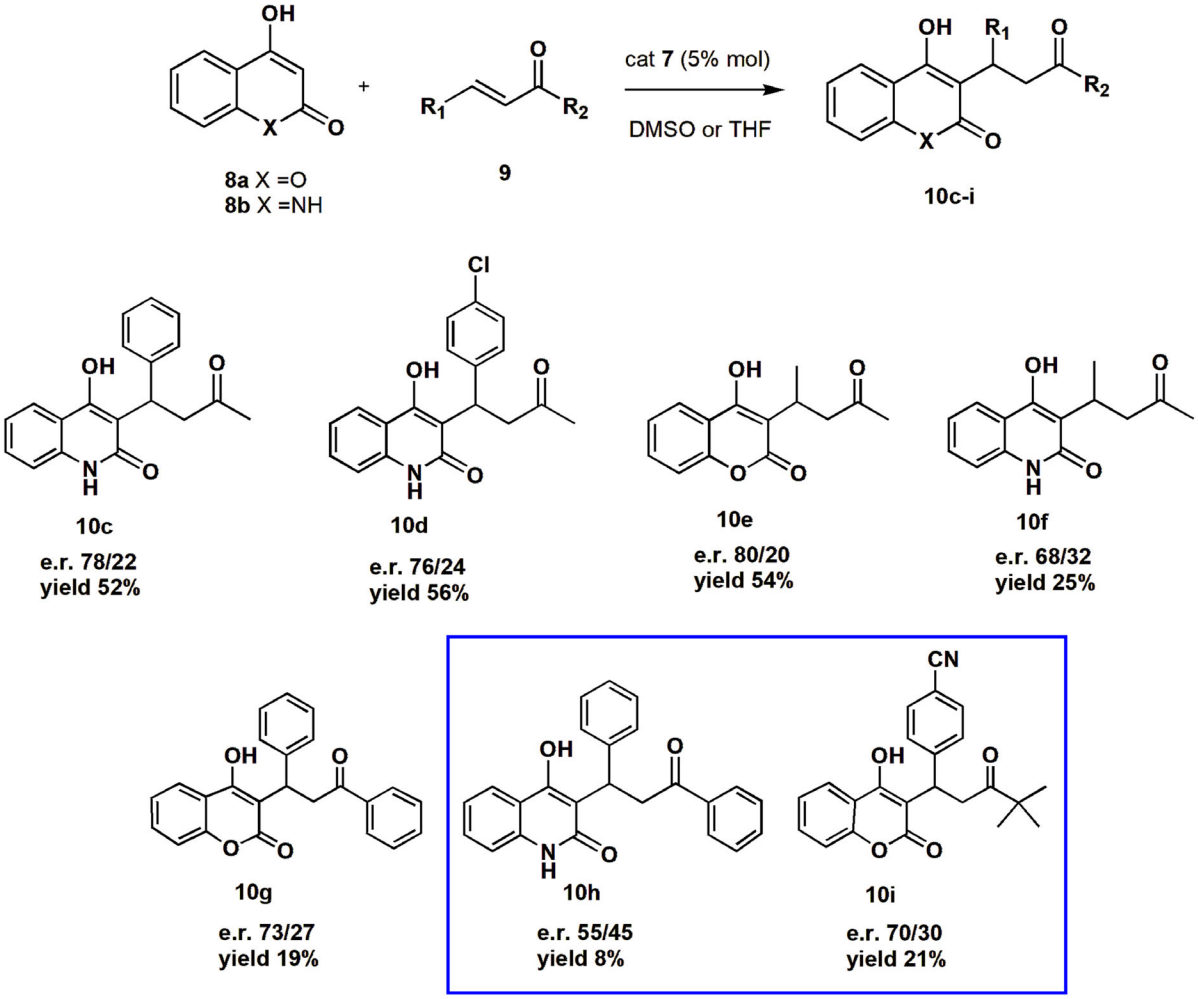

Figure 4. Reactions between 4-hydroxycoumarin (**8a**)/4-hydroxyquinolin-2-one (**8b**) and α,β-unsaturated ketones catalyzed by (*all-R*)-**7.** Structure of obtained compounds and the corresponding enantiomeric ratio/yield. In the blue box, novel synthesized compounds. The reactions were performed with **8** (0.2 mmol), **9** (0.24 mmol), solvent (2 mL), at room temperature, 48 h. Yield refers to the isolated product after column chromatography. Enantiomeric ratio was determined by chiral HPLC.

Research Article
doi.org/10.1002/ejoc.202500338

analysis of a simplified reaction mixture where the α,β-unsaturated ketone **9b** has been reacted with catalyst (*all-R*)-**7**. The reaction allows the formation of three expected imine intermediates in reasonable abundances after 30 min of reaction starting at room temperature (data not shown). High-resolution mass spectral data supported the proposed structures of intermediates as reported in **Figure 5**. In details, after 2 h, the signal corresponding to the mono-imine intermediate (m/z 913.4737, $\Delta m/z = 2.0$ ppm) was detectable and it exhibited highest intensity, followed by the signal correlated with the bis-imine (m/z 1075.4979, $\Delta m/z = 2.2$ ppm) while the signal corresponding to the tris-imine (m/z 1237.5222, $\Delta m/z = 2.4$ ppm) species has the lowest intensity. This fast experiment proves that each DPEDA-based unit works independently in the catalytic process.

2.3. Scale-Up Evaluation

Coumachlor is a first-generation rodenticide used in many countries but also used as a pesticide and as building block in chemical synthesis. As for the warfarin, coumachlor is marketed as racemates although the (S)-enantiomer has been proven to be more active than the (R)-enantiomer. To verify our procedure, we performed scale-up synthesis using 4-hydroxy-chromen-2-one **8a** (1 g, 6.20 mmol) and **9b** (1.34 g, 7.44 mmol) under the same standard reaction conditions. To our delight, product **10b** was generated in high yield (83%) with good enantiomeric ratio (80/20).

2.4. Reuse of Catalyst

The recyclability and reuse of the *all-(R)*-**7** catalyst was also evaluated being a critical challenge in homogeneous phase due to the frequent decomposition or loss of the catalyst. In the synthesis of coumachlor **10b**, we attested the activity of the catalyst over three consecutive reaction cycles (at mg scale). After each reaction, the catalyst was recovered by column chromatography washing with methanol. The recovered catalyst was ≈80% and its integrity was confirmed by ^{1}H-NMR analysis before the subsequent reaction. Yield and enantioselectivity were maintained in the first two cycles (95% and 79/21 e.r. (R/S) respectively) while after the third cycle, a little decrease of yield was recorded (89%) without loss of stereoinduction ability. Unfortunately, after the third cycle, the catalyst was deactivated.

2.5. Antioxidant Activity

4-hydroxycoumarin and 4-hydroxyquinolin-2-one derivatives have attracted great attention due to their biological properties. These scaffolds are present in many classes of natural products and pharmaceuticals.[42,43] Notably, they display radical scavenging capability, and recent works report on the novel derivatives of hydroxycoumarins and hydroxyquinoline.[44–48] The synthetized compounds (as enantioenriched sample) were tested by the DPPH$^{\bullet}$ and ABTS$^{\bullet+}$ radical assays following standard protocols as reported in the experimental section. As a first fast screening, all compounds were evaluated to inactivate both reactive radical species at 1 mM (see Supporting materials). Only four compounds gave significant score against ABTS$^{+\bullet}$ (% inhibition > 50), and then their IC_{50} values were determined (**Table 2**). None of the compounds showed significant activity against DPPH$^{\bullet}$. Specifically, a good scavenging effect was recorded for **10c** and **10f** which are both quinoline-2-one derivatives, though the scavenging potency was 20 times lower than that of ascorbic acid. Looking at the chemical structures of **10e** and **10f**, the presence of nitrogen instead of oxygen appears relevant for the activity (**10e** exhibits a 60-fold lower potency compared to ascorbic acid) and the sale holds true for presence of the acetyl group (in the case of **10 h** the activity collapse, inhibition of 26% at 1 mM, table S1,

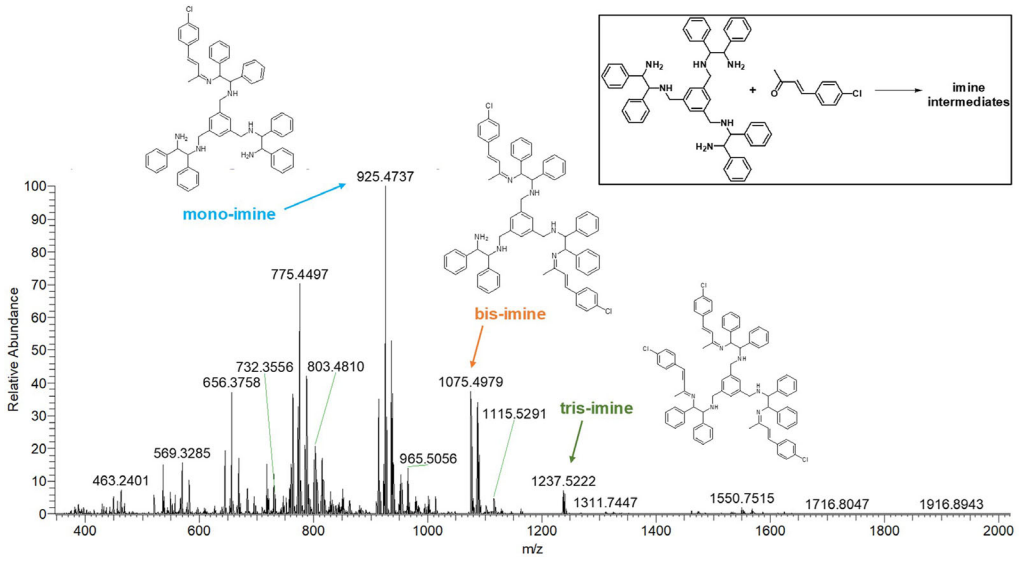

Figure 5. HR-ESI-MS spectrum of ketone **9b** and catalyst (*all-R*)-**7** mixture over time (structure of reagents in the box). Total ion current (TIC) spectrum of reaction after 2 h. The detected species include mono-imine (m/z 913.4737), bis-imine (m/z 1075.4979), and tris-imine (m/z 1237.5222) intermediates, confirming the stepwise activity of the multiple amine units.

Research Article
doi.org/10.1002/ejoc.202500338

Table 2. IC_{50} of ABTS•$^{+}$ radical scavenging activity of the most active compounds.

Compound	IC_{50} [mM]
Ascorbic acid	0.007 ± 0.002
10c	0.131 ± 0.016
10f	0.139 ± 0.059
10d	0.318 ± 0.060
10e	0.363 ± 0.063

Supporting Information). The inability of these compounds to effectively scavenge the DPPH radical may stem from their specific antioxidant mechanism. DPPH•, a stable, lipophilic free radical, primarily reacts via hydrogen atom transfer and is susceptible to steric hindrance, limiting its reactivity with hydrophilic molecules. Conversely, ABTS•+, a radical cation, predominantly reacts through electron transfer, readily interacting with electron donors and exhibiting less sensitivity to steric hindrance, thus enabling it to react with a broader range of antioxidants. Therefore, based on these observations, we propose that the newly synthesized molecules exert their antioxidant activity predominantly through electron transfer mechanisms.

3. Conclusion

Aiming to extend the portfolio of chiral amino-based organocatalysts with C_3-symmetry, we prepared two symmetric enantiopure diphenylethylendiamine-based catalysts in a few steps. These catalysts were tested in specific Michael additions of α/β unsaturated ketones with 4-hydroxycoumarin focusing the optimization reaction conditions to the warfarin and coumachlor production. The structure of catalyst bearing all-amino groups provided the best results in terms of yield and stereoinduction (up to 95% yield and 80/20 e.r.). In addition, a small library of compounds was obtained using also the 4-hidroxyquinolin-2-one as Michael acceptor, and the DPPH$^{\cdot}$ and ABTS•$^{+}$ radical scavenging assays were conducted as the first biological tests. Notably, although in low yields, two products were synthesized for the first time. Finally, to explore the scalability of the catalyst, coumachlor was synthetized in gram-scale, and the catalyst was recovered and reused three times without loss in yield and stereoselectivity.

4. Experimental Section

All commercial reagents, solvent used for analysis, and HPLC solvent were purchased from Sigma Aldrich, Fluorochem or BLD pharm. For column chromatography, silica gel 60 Å (230-400 mesh) from Sigma Aldrich was used. The thin layer chromatography used to monitor the reaction was using Merck TLC Silica gel 60 F254 aluminum sheets, then UV light (254 nm) was used for visualization. NMR spectra were recorded at 298 K by Bruker AM 400 in $CDCl_3$, MeOH-d_4, and DMSO-d_6 except spectra of one sample were recorded by Bruker AM 300. Coupling constants were reported in Hz. HR-MS spectra were obtained on Orbitrap Exactive Instrument (Thermo Fischer). Optical rotation [α] was measured by a Jasco P1030 Polarimeter at specific temperature. Isolation of enantiomers was performed by HPLC JASCO equipped with UV and CD detections. All the reported product yields were calculated based on pure material isolated after column purification.

Computational Analysis

Calculations performed to conduct the conformational analysis of compounds **6** and **7**, both in (*all-R*) configuration, and to model the transition states $\mathbf{TS_a}$, $\mathbf{TS_b}$, $\mathbf{TS_c}$, and $\mathbf{TS_d}$ quoted in the main text and reported in Figure S30 within Supporting Information have been conducted by means of the computer program Spartan 10v110 (Wavefunction Inc., 18401 Von Karman Avenue, Suite 370, Irvine, CA 92612, USA), according to the steps listed below.

Conformational Analysis of Compounds 6 and 7

In step 1, the geometries characterizing the catalysts **6** and **7** have been initially submitted to conformational search at the molecular mechanics level of theory (used force field: MMFF94). In step 2, the 50 obtained more stable conformers of **7**, inside an energy range of 7.3 kJ, and the 50 obtained more stable conformers of **6**, inside an energy range of 6.3 kJ, were then submitted to further energy optimization by semiempirical approach with the PM6 Hamiltonian.

Optimization of TS Geometries Generated by Reaction between Catalyst 7 and Ketone 9a Leading to the Formation of the Related Carbinolamine

Four independent transition state geometries $\mathbf{TS_a}$, $\mathbf{TS_b}$, $\mathbf{TS_c}$, and $\mathbf{TS_d}$ have been assembled by hand by disposing catalyst **7** in presence of both one hydroxyquinoline **8a** and one ketone **9a** molecules, according to the supramolecular disposition reported in Figure S30 of Supporting Information. All these were then optimized at the PM6 semiempirical level of theory, according to the "Transition State Geometry" algorithm implemented within Spartan program. All the optimized **TS** structures were validated as true saddle points by checking the presence among the assessed vibrational modes of only one imaginary frequency (such values have been inserted within Figure S30 and Table S1, Supporting Information). Each of the $\mathbf{TS_a}$, $\mathbf{TS_b}$, $\mathbf{TS_c}$, and $\mathbf{TS_d}$ structures has been also submitted to single point energy calculation at two different DFT levels of theory: 1) B3LYP/6-31 G*; 2) M06/6-31 G*.

DPPH Radical Scavenging Assay

The 2,2-diphenyl-1-picrylhydrazyl (DPPH$^{\cdot}$) was dissolved in ethanol to reach a final concentration of 120 μM. The mixture was vortexed and subsequently diluted with ethanol to achieve an absorbance value of 0.7 at 517 nm. To 196 μL of DPPH• solution, 4 μL of each sample (50 mM in DMSO) at final concentration of 1 mM was added. The reaction was allowed to proceed in the dark at room temperature for 15 min, and absorbance values were recorded at 517 nm using DMSO as a blank. The percentage inhibition at 1 mM for each tested molecule was calculated relative to the blank. Ascorbic acid at 1 mM was used as a positive control. The experiments were conducted at least two times ($n = 2$).

ABTS•$^{+}$ Radical Scavenging Assay

The 2,2′-azinobis-(3-ethylbenzothiazoline-6-sulfonic acid) diammonium salt (ABTS-$(NH_4)_2$) was dissolved in water to reach a final concentration of 7 mM. The ABTS radical cation (ABTS•$^{+}$) was generated by adding 2.45 mM potassium persulfate. The mixture was incubated in the dark for 16 h and subsequently diluted with ethanol to achieve

an absorbance value of 0.7 at 734 nm. To 196 μL of ABTS•$^+$ solution, 4 μL of each sample (50 mM in DMSO) at various final concentrations (from 0.0003 to 1 mM) was added. The reaction was allowed to proceed in the dark at room temperature for 6 min, and absorbance values were recorded at 734 nm using DMSO as a blank. The calculated IC 50 values, expressed in mM, were compared with the values obtained from the ascorbic acid calibration curve. The experiments were conducted at least three times ($n = 3$).

Supporting Information

Synthetic procedures, NMR and HPLC characterization data, MS spectra and additional computational data are in Supplementary info.

Acknowledgements

A.C. and G.M. thank PON "RICERCA E INNOVAZIONE" 2014–2020 azione IV.6 "CONTRATTI DI RICERCA SU TEMATICHE GREEN" for funding this research work. A.C. thanks the PNRR PE6 project (SPOKE5 WP.4) for research funds.

Open access publishing facilitated by Universita degli Studi di Roma La Sapienza, as part of the Wiley - CRUI-CARE agreement.

Conflict of Interest

The authors declare no conflict of interest.

Data Availability Statement

The data that support the findings of this study are available in the supplementary material of this article.

Keywords: asymmetric reaction · Michael additions · organocatalysis · warfarin

[1] a) A. Nakamura, M. Tsutsui, *Principles and Applications of Homogeneous Catalysis*, Wiley, New York **1980**; b) R. Noyori, *Asymmetric Catalysis in Organic Synthesis*, Wiley, New York **1994**; c) B. List, J. W. Yang, *Science* **2006**, *313*, 1584; d) M. Hönig, P. Sondermann, N. J. Turner, E. M. Carreira, *Angew. Chem. Int. Ed.* **2017**, *56*, 8942.
[2] a) S. K. Sharma, A. S. R. Paniraj, Y. B. Tambe, J. Agric, Food Chem. **2021**, *69*, 14761; b) M. De Angelis, C. Sappino, E. Mandic, M. D'Alessio, M. G. De Dominicis, S. Sannino, L. Primitivo, P. Mencarelli, A. Ricelli, G. Righi, *Tetrahedron* **2021**, *79*, 131837.
[3] M. R. Monaco, B. Poladura, M. Diaz de Los Bernardos, M. Leutzsch, R. Goddard, B. List, *Angew. Chem. Int. Ed.* **2014**, *53*, 7063.
[4] a) C. A. Denard, J. F. Hartwig, H. Zhao, *ACS Catal.* **2013**, *3*, 2856; b) J. Alemán, S. Cabrera, *Chem. Soc. Rev* **2013**, *42*, 774.
[5] Y. Zou, Z.-C. Huang, M. Xiang, C.-Y. Li, X. Li, F. Tian, L.-X. Wang, *J. Org. Chem.* **2021**, *86*, 17371.
[6] O. Pàmies, J. E. Bäckvall, *Adv. Synth. Catal.* **2002**, *344*, 915.
[7] S. V. Kochetkov, A. S. Kucherenko, S. G. Zlotin, *Org. Biomol. Chem.* **2018**, *16*, 6423.
[8] Y. Qin, L. Zhu, S. Luo, *Chem. Rev.* **2017**, *117*, 9433.
[9] P. Kisszékelyi, Z. Fehér, S. Nagy, P. Bagi, P. Kozma, Z. Garádi, M. Dékány, P. Huszthy, B. Mátravölgyi, J. Kupai, *Symmetry* **2021**, *13*, 521.
[10] V. Kozel, C. G. Daniliuc, P. Kirsch, G. Haufe, *Angew. Chem. Int. Ed.* **2017**, *56*, 15456.
[11] M. Antonijevic, C. Rochais, P. Dallemagne, *Molecules* **2023**, *28*, 679.
[12] L.-I. Rodríguez, T. Roth, J. L. Fillol, H. Wadepohl, L. H. Gade, *Chem. Eur. J.* **2012**, *18*, 3721.
[13] M. Yamanaka, T. Nakagawa, R. Aoyama, T. Nakamura, *Tetrahedron* **2008**, *64*, 11558.
[14] C. V. Crişan, A. Soran, A. Bende, N. D. Hădade, A. Terec, I. Grosu, *Molecules* **2020**, *25*, 3789.
[15] M.-H. Yu, X.-T. Liu, B. Space, Z. Chang, X.-H. Bu, *Coord. Chem. Rev.* **2021**, *427*, 213518.
[16] M. A. Alshubramy, K. A. Alamry, M. A. Hussein, *RSC Adv.* **2023**, *13*, 14317.
[17] G. Kuppadakkath, S. S. Jayabhavan, K. K. Damodaran, *Molecules* **2024**, *29*, 2149.
[18] J. Han, H. Wu, M. Teng, Z. Li, Y. Wang, L. Wang, Y. Pan, *Synlett* **2009**, *6*, 933.
[19] J. N. Moorthy, S. Saha, *Eur. J. Org. Chem.* **2010**, *33*, 6359.
[20] K. Murai, S. Fukushima, S. Hayashi, Y. Takahara, H. Fujioka, *Org. Lett.* **2010**, *12*, 964.
[21] K. Murai, A. Nakamura, T. Matsushita, M. Shimura, H. Fujioka, *Chem. Eur. J.* **2012**, *18*, 8448.
[22] A. Sorato, M. De Angelis, S. Badasa Oljira, M. Pierini, G. Mazzoccanti, M. P. Donzello, A. Ciogli, *ChemCatChem* **2024**, *16*, e202400031.
[23] S. B. Oljira, M. De Angelis, A. Sorato, G. Mazzoccanti, S. Manetto, I. D'Acquarica, A. Ciogli, *Catalysts* **2024**, *14*, 915.
[24] L. W. Xu, J. Luo, Y. Lu, *Chem. Commun.* **2009**, *14*, 1807.
[25] N. Halland, T. Hansen, K. A. Joergensen, *Angew. Chem, Int. Ed.* **2003**, *42*, 4955.
[26] H. Kim, C. Yen, P. Preston, J. Chin, *Org. Lett.* **2006**, *8*, 5239.
[27] J. W. Xie, L. Yue, W. Chen, W. Du, J. Zhu, J. G. Deng, Y. C. Chen, *Org. Lett.* **2007**, *9*, 413.
[28] Z. Dong, L. Wang, X. Chen, X. Liu, L. Lin, X. Feng, *Eur. J. Org. Chem.* **2009**, *2009*, 5192.
[29] A. S. Kucherenko, V. G. Lisnyak, A. O. Chizhov, S. G. Zlotin, *Eur. J. Org. Chem.* **2014**, *18*, 3808.
[30] R. Porta, M. Benaglia, F. Coccia, S. Rossi, A. Puglisi, *Symmetry* **2015**, *7*, 1395.
[31] T. Shi, Z. Guo, H. Yu, J. Xie, Y. Zhong, W. Zhua, *Adv. Synth. Catal.* **2013**, *355*, 2538.
[32] M. De Angelis, M. Managò, F. Pepi, C. Salvitti, A. Troiani, C. Villani, A. Ciogli, *RSC Adv.* **2024**, *14*, 1576.
[33] The calculated pka of 4-hydroxyquinolin-2-one was 7.31 (Marvin software). The pka of 2,4-dihydroxyquinolone is 5.9 in A. Albert, J.N. Philips, *J. Chem. Soc.* **1956**, 1294.
[34] G. Mazzoccanti, O. H. Ismail, I. D'Acquarica, C. Villani, C. Manzo, M. Wilcox, A. Cavazzini, F. Gasparrini, *Chem. Commun.* **2017**, *53*, 12262.
[35] C. Eswaran, A. Rajendran, S. Krishanu, N. Ramalingam, S. Palani, *Adv. Synth. Catal.* **2020**, *362*, 1144.
[36] P. Geetika, R. Ashok, K. Namrata, K. Manish, D. Utpal, S. Rohit, B. Subhash, *Chemistry Select* **2024**, *9*, e202401457.
[37] Z. Chen, H. Li, Y. Liao, M. Wanga, W. Su, *Chem. Commun.* **2023**, *59*, 6686.
[38] C. Iacobucci, S. Reale, F. De Angelis, *Angew. Chem. Int. Ed.* **2016**, *55*, 2980.
[39] J. Mehara, J. Roithová, *Chem. Sci.* **2020**, *11*, 11960.
[40] A. Iazzetti, G. Mazzoccanti, G. Bencivenni, P. Righi, A. Calcaterra, C. Villani, A. Ciogli, *Eur. J. Org. Chem.* **2022**, *2022*, e202101272.
[41] A. Arcadi, G. Berden, A. Ciogli, D. Corinti, M. E. Crestoni, M. De Angelis, G. Fabrizi, A. Goggiamani, A. Iazzetti, F. Marrone, V. Marsicano, J. Oomens, A. Serraiocco, *RSC Adv.* **2023**, *13*, 10090.
[42] K. Proisl, S. Kafka, J. Kosmrlj, *Current Organic Chemistry* **2017**, *21*, 1949.
[43] J.-C. Jung, O.-S. Park, *Molecules* **2009**, *14*, 4790.
[44] E. H. Avdović, Z. Milanović, *Antioxidants* **2023**, *12*, 2070.
[45] B. Rostom, E. Goya-Jorge, L. V. Muro, I. Boubrik, S. Wiorek, R. Karaky, I. Kassab, M. E. J. Rodríguez, M. Sylla-Iyarreta Veitía, *Can J Physiol Pharmacol.* **2024**, *102*, 361.
[46] I. Mieriņa, A. Stikute, M. Jure, *Tetrahedron Letters* **2022**, *99*, 153847.
[47] T. Khamkhenshorngphanuch, K. Kulkraisri, A. Janjamratsaeng, N. Plabutong, A. Thammahong, K. Manadee, S. Pombejra, T. Khotavivattana, *Molecules* **2020**, *25*, 3059.
[48] D. Li, N. Oku, Y. Shinozaki, Y. Kurokawa, Y. Igarashi, *Beilstein J. Org. Chem.* **2020**, *16*, 1489.

Manuscript received: June 10, 2025
Revised manuscript received: June 30, 2025
Version of record online: